

Displacement-based selection of ground motion records for efficient seismic response analysis

M. Brozovič & M. Dolšek

University of Ljubljana, Slovenia



SUMMARY:

The issue of the number of records required for sufficiently accurate prediction of seismic response of a structure can be partly solved by using the precedence list of ground motion records, which make it possible to calculate the response of structure progressively, starting from the first ground motion record from the precedence list, until desired tolerance is achieved. Herein the efficiency of the precedence list of records, if determined based on acceleration spectrum or inelastic response of simple model, is investigated for the example of an eight-storey reinforced concrete frame building. It is shown that the precedence list of records, which utilize inelastic response of simple model, is more efficient in terms of predicting response parameters of the building.

Keywords: precedence list, ground motion, record selection, progressive incremental dynamic analysis

1. INTRODUCTION

Many procedures for selection of ground motion records on the basis of different criteria have been developed, as discussed by Katsanos et al. (2010). The most basic procedures for selection of records involve criteria associated with the earthquake magnitude and distance of the rupture zone from the location of the building of the interest. However, these procedures were not found to be very efficient in terms of nonlinear response of structure (Iervolino and Cornell, 2005). Thus selection of ground motion records based on magnitude and distance is often enhanced by spectral matching. This approach is adopted in the codes for seismic-resistant design of building, e.g. in Eurocode 8 (CEN, 2004a), which prescribes that the uniform hazard spectrum should be used as a target spectrum, but such approach is conservative. Baker (2011) proposed an alternative target spectrum, termed a conditional mean spectrum (CMS). He showed that structural responses from ground motions matching the more probabilistically consistent conditional mean spectrum are significantly smaller than the response from ground motion matching the uniform hazard spectrum. However, Bradley (2010) identified limitation of the CMS approach and proposed a generalized conditional intensity measure approach (GCIM) that allows determination of the conditional distribution of any arbitrary ground-motion intensity measure.

Although many ground-motion selection procedures exist, usually they do not address the issue of number of records required for sufficiently accurate prediction of seismic response of a structure. This issue was partly solved by introducing precedence list of ground motion records, which was firstly used for progressive incremental dynamic analysis (IDA) (Vamvatsikos and Cornell, 2002, Azarbakht and Dolšek, 2007, 2011). In progressive IDA, the IDA curves are computed progressively, starting from the first ground motion record in the precedence list. Once the acceptable tolerance is achieved the analysis can be terminated. Computational efficiency of progressive IDA depends on the procedure used to define the precedence list of ground motion records.

Different procedures for determination of precedence list of ground motion records were thus examined in the study presented in this paper. Precedence lists of ground motion records were

determined by utilizing elastic acceleration spectra, the IDA analysis performed for the SDOF model and web-based approximate IDA (Peruš et al., 2012). The efficiency of these precedence lists of ground motion records, which make it possible to predict seismic response by the small number of records, is demonstrated by means of seismic performance assessment of an eight-storey reinforced concrete frame building.

2. PRECEDENCE LIST OF GROUND MOTION RECORDS

Precedence list of ground motion records has been proposed aiming at minimizing the computational time, which is required for sufficiently accurate prediction of seismic response parameters in the case if they are estimated with nonlinear response history analysis (Azarbakht and Dolšek 2007, 2011). The determination of such a list is an optimization problem and can be solved by minimizing the fitness function, which can be based on different criteria. For example, fitness function can be defined on the basis of spectral acceleration or, as originally proposed, on the basis of response of a simple model, e.g. the single-degree-of-freedom (SDOF) model.

The methodology for determination of the precedence list of records was originally proposed for prediction of median seismic response (i.e. median IDA curve) (Azarbakht and Dolšek, 2007). Recently, progressive IDA for first-mode dominated structures was introduced. It involves precedence list appropriate for predicting 16th, 50th and 84th percentile response (Azarbakht and Dolšek 2011). The benefit of progressive IDA, in comparison to the IDA, is the reduction of the computational effort. However, determination of the precedence list of ground motion records also requires some computational time, whereas the efficiency of the precedence list of ground motion depend on the fitness function, optimization technique, and the structure under consideration. In the case if determination of precedence list of ground motion records involves IDA analysis of the simple model (e.g. SDOF model) then the computational time needed for determination of precedence list is usually shorter than time needed for determination of one IDA curve of a structure.

The precedence list of ground-motion records is determined by rearranging the ID numbers of the ground-motion records in order to minimize the fitness (objective) function, which is for the purpose of this study defined on the basis of acceleration spectra or on the basis of inelastic response of equivalent SDOF model. In general, the fitness functions can be defined for different purposes. However, for the precedence list of ground motions aiming at predicting the fractile IDA curves (e.g. 16th, 50th and 84th percentile IDA curve), it was found (Azarbakht and Dolšek 2011), that a good measure for defining the fitness function is the area between the “original” fractile IDA curve and the “selected” fractile IDA curve. Note that the term “original” is used for the case if fractile IDA curve is obtained from all the IDA curves, while the term “selected” is used if the fractile IDA curve is determined only for the first s ground motions from the precedence list. If the area between the “original” and “selected” fractile IDA curve area is normalized with the area defined by the “original” fractile IDA curve then the dimensionless measure for the error between the two types of the fractile IDA curves can be defined as follows

$$Error(s, f) = 100 \times \frac{\int_0^{EDP_{\max}(s, f)} |\Delta IM(s, f)| dEDP}{\int_0^{EDP_{\max, or}(f)} IM_{or}(f) dEDP} \quad (2.1)$$

where s is the number of selected subsets of three ground motions, IM and EDP are usual notations for intensity measure and engineering demand parameter, respectively, $IM_{or}(f)$ is the intensity measure of the “original” f -th percentile IDA curve, $EDP_{\max, or}(f)$ is the engineering demand parameter corresponding to the capacity point of the “original” f -th percentile IDA curve, $\Delta IM(s, f)$ is the difference in the IM corresponding to the “original” and “selected” f -th percentile IDA curve, and

$EDP_{max}(s,f)$ is the maximum of the engineering demand parameters corresponding to the capacity point of the “selected” and “original” f -th percentile IDA curves.

In addition to the *Error* (Eqn. 2.1), which is defined on the basis of inelastic response of the simple model, we defined the error between “selected” and “original” fractile spectral acceleration, as follows

$$Error(s, f) = 100 \times \frac{\int_{T_{min}}^{T_{max}} |\Delta S_a(s, f)| dT}{\int_{T_{min}}^{T_{max}} S_{a,or}(f) dT} \quad (2.2)$$

where T_{min} and T_{max} are periods defining lower and upper limit of the integrals, $S_{a,or}(f)$ is spectral acceleration at the period T of the “original” f -th percentile spectral acceleration and $\Delta S_{a,or}(s, f)$ is the difference in the S_a corresponding to the “original” and “selected” f -th percentile spectral acceleration.

In order to define the fitness function the sum of $Error(s, f)$ over all values is required. In the case if the precedence list of ground motions is determined to predict the three percentile IDA curves it was found (Azarbakht and Dolšek 2011), that the best precedence list is obtained if the fitness function is defined in a way to give a preference to those ground motions, which IDA curves are close to the “original” fractile curves. Therefore, the fitness function Z is defined by sum of $Error(s, f)$ over the m number of subsets of ground motion records and over the three percentile IDA curves

$$Z = \frac{1}{m} \sum_{s=1}^m \sum_{f=1}^3 Error(s, f) \quad (2.3)$$

Different techniques can be used to minimize the fitness function. The simplest possible way, which actually does not require optimization method, is gradual minimization of $Error(s, f)$. It was proven that gradual minimization of $Error(s, f)$ results in a value of the fitness function, which is close to the global minimum (Azarbakht and Dolšek, 2011). In this case the first ground motion in the precedence list corresponds to the minimum value of errors (Eqn. 2.1 or 2.2) that are calculated for $s=1, f=1$ and for all n records in the given set of ground motion records. The second and third ground motion in the precedence list correspond to minimum error calculated for $s=1, f=2$ and $f=3$ for $n-1$ and $n-2$ records left to be placed in the precedence list, respectively. The following ground motion IDs in the precedence list are defined with repeating described procedure until all ground motion IDs are placed in the precedence list of ground motions.

Obviously, determination of precedence list of records based on acceleration spectra is less complicated than the procedure, which involves response of the SDOF model defined on the basis of the pushover analysis. In this study it was defined that the lateral loads used in the pushover analysis corresponded to the product of mass matrix and the mode shape vector, which has the value 1 at the location of the top displacement. For all cases presented herein pushover analysis is based on the fundamental mode shape vector. Result of the pushover analysis is pushover curve, a relationship between the base shear F and the top displacement D .

An idealization of the base shear – top displacement relationship is required in order to define force-displacement relationship of an equivalent SDOF model, which was used for determination of approximate IDA curves. The pushover curve was thus idealized by the quadrilinear relationship (Fig. 1), which shape can be described by the four dimensionless parameters (r_v, r_h, μ_u, α) of the pushover curve (Peruš et al. 2012). These parameters were defined as

$$r_v = \frac{F_1}{F_2}, \quad r_h = \frac{u_1}{u_2}, \quad \mu_u = \frac{u_3}{u_2}, \quad \alpha = -\frac{k_{pc}}{k_1} \quad (2.4)$$

where pairs (u_1, F_1) and (u_2, F_2) represent first and the second characteristic point of the idealized force-displacement relationship and roughly represent the cracking of concrete and, in the case of regular structures, yielding of reinforcements at the base of columns, respectively. The displacement u_3 is related with the displacement where the strength of the structure starts degrading, while for the corresponding force F_3 the same value as for F_2 is assumed. Parameters k_{pc} and k_1 are the post-capping and initial stiffness of the idealized force-displacement relationship, respectively.

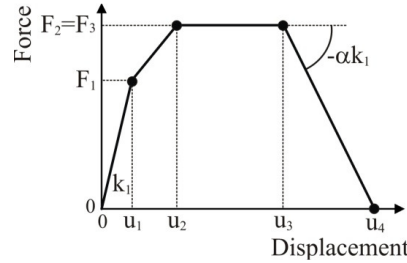


Figure 1. The idealized base shear – top displacement of the pushover curve

The force-displacement of the equivalent SDOF model (F^* and D^*) was determined by dividing the base shear F and top displacement D of the idealized pushover curve with the transformation factor Γ , which was defined as follows

$$\Gamma = \frac{m^*}{\sum_{i=1}^n m_i \phi_i^2}, \quad m^* = \sum_{i=1}^n m_i \phi_i \quad (2.5)$$

where m_i and ϕ_i are masses and component of the mode shape vector at the location of the i^{th} storey, and m^* is the mass of the equivalent SDOF model. The quadrilinear force-displacement relationship enables very good idealization of the first part of the pushover curve, where the structural behaviour is still elastic. Therefore the period of the equivalent SDOF model

$$T^* = 2\pi \sqrt{\frac{m^* D_1^*}{F_1^*}} \quad (2.6)$$

is practically the same as the first-mode elastic period T_1 . Thus, we did not distinguish between the period of the equivalent SDOF model and that associated with the mode shape vector used for determination of lateral loads of pushover analysis. Similarly, the ground motion intensity, if characterized by the spectral acceleration corresponding to the first-mode elastic period $S_{ae}(T_1)$ and 5% damping ratio is consistent intensity measure for the case of IDA or approximate IDA, which involves response of the SDOF model.

The approximate IDA curves associated with the equivalent SDOF model were basically determined by performing nonlinear response history analysis of an equivalent SDOF model but for the comparison reasons also by using recently developed web-application for prediction of approximate IDA curves (Peruš et al. 2012).

3. DESCRIPTION OF AN EIGHT STOREY BUILDING, MATHEMATICAL MODELLING AND GROUND MOTIONS

An eight-storey building (Fig. 2) was designed according to the Eurocode 8 (Kosič, 2010). The building's height of the first and second storeys is 5 m, whereas the height of other storeys is 3.1 m. All the cross-sections of the columns and beams of the structure have dimensions of 60/60 cm and

40/60 cm, respectively. The reinforcement of the columns is the same for all sections, except for the cross-sections of the columns at the base, where the density of the stirrups is greater ($\Phi 8/5$ cm and $\Phi 10/5$ cm). The top of the beams in first two storeys are reinforced with $6\Phi 20$, whereas all other beams are reinforced as presented in Fig. 2. The concrete strength class of the building is C30/37, and the steel strength class is B500.

Structural models of the buildings were prepared in PBEE toolbox (Dolsek 2010) in conjunction with OpenSEES (2007). Beam and column flexural behaviour was modelled by one-component lumped plasticity elements, consisting of an elastic beam and two inelastic rotational hinges. The moment-rotation relationship before strength deterioration was modelled by a bi-linear relationship, whereas the post-capping stiffness was assumed to be linear, with a descending branch. The yield and maximum moment in the columns were calculated taking into account the axial forces due to the vertical loading. The ultimate rotation Θ_u in the columns at the near collapse (NC) limit state corresponded to 80% of the maximum moment measured in the post-capping range of the moment-rotation relationship. It was estimated by means of the Conditional Average Estimate (CAE) method (Peruš et al., 2006). For the beams, the EC8-3 (CEN, 2005) formulas were used to compute the ultimate rotations in the plastic hinges. The masses were concentrated at the storey levels, at the centre of gravity and the effective width of the beams was modelled as described in Eurocode 2 (CEN, 2004b), assuming zero moment points at the midpoint of the beams. Nonlinear dynamic analyses were performed by assuming 5 % damping proportional to mass.

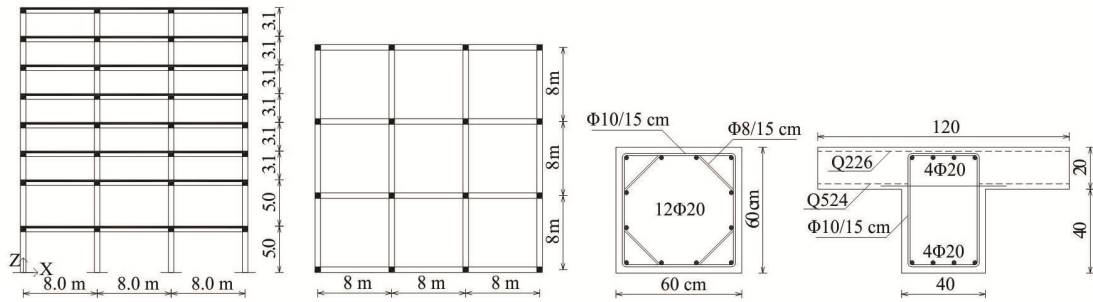


Figure 2. The elevation, plan view and reinforcement in cross-sections of the columns and beams of the building

A set of records consisted of 30 ground motion records used in previous study (Vamvatsikos, Cornell, 2006). The records have been selected within events having a magnitude between 6.5 and 6.9. All the ground motion records have been recorded on firm soil, with a distance range from the epicentre of 12 - 55 km. The acceleration spectra normalised to the spectral acceleration at fundamental time period of the building ($T_1 = 1.76$ s) are presented in Fig. 3 for each ground motion records, and the corresponding 16th, 50th and 84th percentiles.

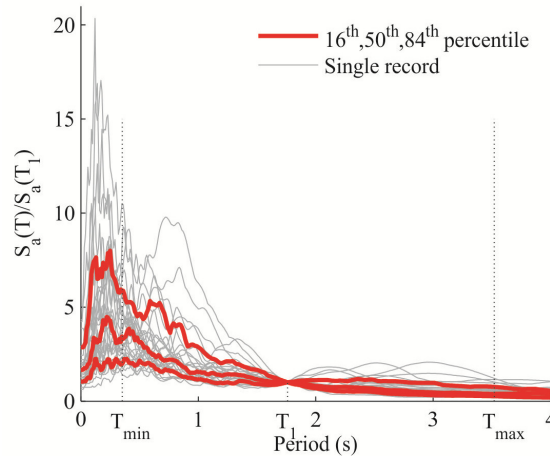


Figure 3. Acceleration spectra for 30 ground motion records and corresponding 16th, 50th and 84th percentiles

4. RESULTS AND DISCUSSION

4.1. The “selected” and “original” fractile IDA curves

Three different precedence lists were determined based on simple procedure of gradual minimization of *Error* in order to analyse their efficiency. The first precedence list was defined by utilizing elastic acceleration spectra in the range of periods from $T_{\min}=0.2 \times T_1$ and $T_{\max}=2 \times T_1$ as indicated in Fig. 3. The second and third precedence lists were defined on the basis of seismic response of simplified (single-degree-of-freedom, i.e. SDOF) model by using web-based approximate IDA curves and SDOF-IDA curves, respectively. For these cases, the force-displacement envelope of the equivalent SDOF model was determined from the pushover curve, which is shown in Fig. 4 together with idealized force-displacement relationship and the corresponding input parameters of the web-application (Peruš et al. 2012). In order to demonstrate the efficiency of progressive IDA for definition of fractile IDA curves in the case of 30 records, the fourth precedence list was defined by using “exact” IDA curves computed based on the response of the structure. Therefore the fourth precedence list served as point of comparison.

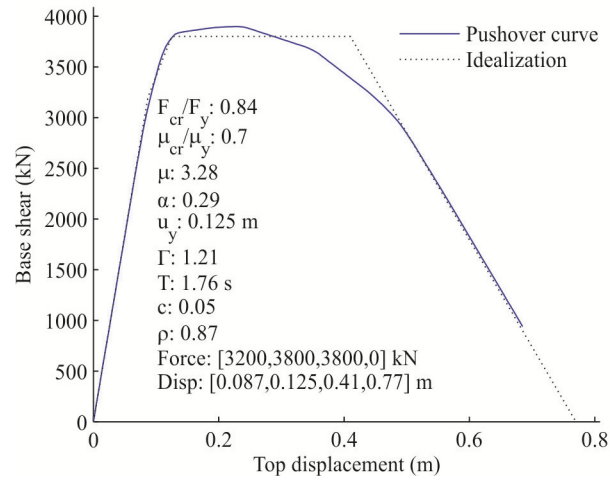


Figure 4. The pushover curve, the idealized force-displacement relationship and the input parameters for determination of the web-based approximate IDA curves

In Fig. 5 “original” and “selected” 16th, 50th and 84th percentile IDA curves are presented for first four subsets of three records from the precedence lists ($s=4$, 12 records) and for all four precedence lists, which were determined by using the gradual minimization of *Error*. Obviously, “selected” fractile IDA curves are in this case presented for only 40 % of records. It can be observed that “selected” fractile IDA curves based on the fourth precedence list (Fig. 5d) practically do not differ to the “original” fractile IDA curves. Thus the percentiles of the maximum storey drifts of this eight-storey building could be efficiently predicted based on only 12 records. However, difference between the “selected” and “original” fractile IDA curves is slightly larger if precedence list were determined based on acceleration spectra, web-based approximate IDA or direct IDA analysis for equivalent SDOF model.

The efficiency of precedence lists with respect to the number of records selected from the precedence list is presented in Fig. 6, where *Error* (Eqs. 2.1 or 2.2) is presented as a function of subset of records ($s=1$ to 10) and for the three percentiles of IDA curves. As expected the smallest errors occur in case if precedence list was determined based on “exact” IDA curves (Fig. 6d). For this case *Error* rarely exceeds 5 %, even for $s=1$. The largest *Error*, around 25%, can be observed for $s=1$ for ground motions from the precedence list based on acceleration spectra (Fig. 6a), but there is clear trend of rapid reduction of the *Error* for s between 1 and 4. The efficiency of precedence lists, which were determined by utilizing web-based approximate IDA curves (Fig. 6b) or IDA curve of the equivalent SDOF model (Fig. 6c), is slightly larger. This is most evident for the case if 50th or 84th percentile

drifts are of interest. In this case efficiency of displacement-based precedence lists (Fig. 6b and 6c) for s larger or equal to 4 is of the same order than that observed for precedence list based on the “exact” IDA curves (Fig 6d).

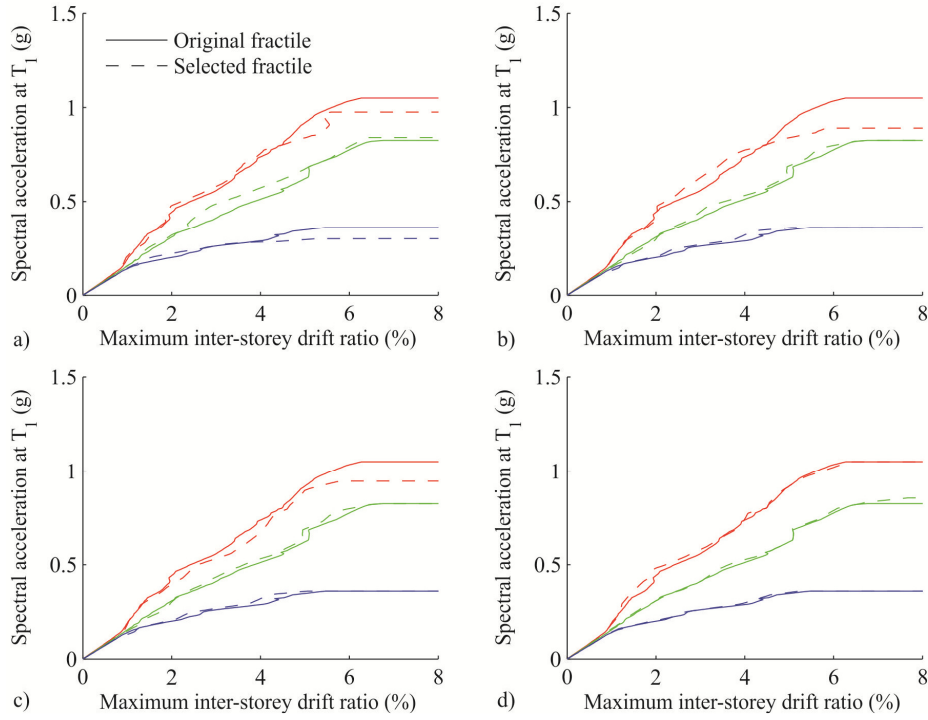


Figure 5. The “original” fractile IDA curves and the “selected” fractile IDA curves ($s=4$: 40 % of records for the precedence list) determined based on a) acceleration spectra, b) web-based approximate IDA curves, c) IDA curves of the equivalent SDOF model and d) “exact” IDA curves

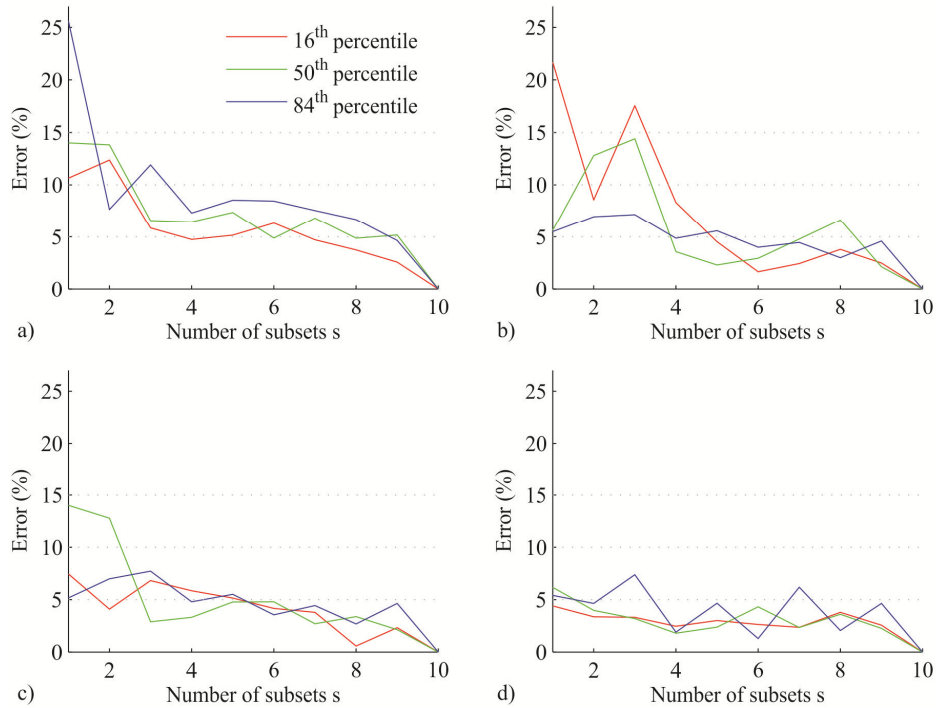


Figure 6. The Error for predicting 16th, 50th and 84th percentile IDA curves on the basis of the precedence list determined by utilizing a) acceleration spectra, b) web-based approximate IDA curves, c) IDA curves of the equivalent SDOF model and d) “exact” IDA curves

4.2. Discussion

If the efficiency of the precedence list of records was measured by the *Error* (Fig. 6) it was shown that the efficiency corresponded to the acceleration-based precedence list is not significantly smaller than that of the displacement-based precedence list. However, more detailed analysis revealed that this is not true. Namely, gradual minimization of *Error* is designed in the way that ground motions have the greatest potential for high places on the precedence list, if the response of the structure for these ground motions is closest to the fractile IDA curves of interest. It is evident that this was optimally achieved if the precedence list was determined base on the “exact” IDA curves. For example, the smallest scatter in IDA curves associated with the 1st, 4th, ..., 28th ground motions from the precedence list, was observed for precedence list based on the “exact” IDA curves (Fig. 7a). However, the same scatter was observed for displacement-based precedence list in the case of SDOF-IDA (Fig. 7b). Slightly larger scatter resulted from the approximate web-based IDA, whereas scatter in IDA curves for the acceleration-based precedence was significantly larger (Fig. 7c). It can be observed that some ground motion from Fig. 7c should be better representatives of 84th percentile IDA curve rather than the 16th percentile IDA curve for which they were selected. Note that the sequences of the ground motion IDs, which were used for determination of IDA curves presented in Fig. 7a and 7b, were slightly different.

Relatively small *Error* based on the acceleration-based precedence list is therefore the consequence of the counting method, which was used for computation of the “selected” fractile IDA curves. Namely, the counting method for determination of the fractile IDA curves does not affect the *Error* if “selected” IDA curve is not similar to the “selected” fractile IDA curve. For example, if odd number of ground motion were selected from the precedence list ($s=1,3,5,\dots$) then the median value corresponded to a certain value on the “selected” IDA curve, whereas in the case if number of ground motion is even, linear interpolation was used between the closest ranks.

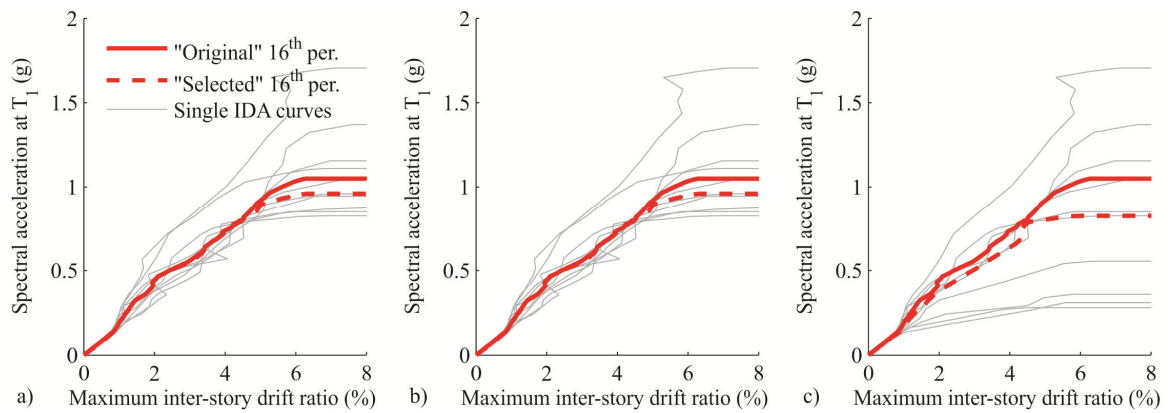


Figure 7. The “original” 16th percentile IDA curve, IDA curves associated with the 1st, 4th, ..., 28th ground motion from the precedence list and the corresponding median IDA curve. All IDA curves are presented for the precedence list based on a) “exact” IDA curves, b) IDA of the equivalent SDOF model or c) acceleration spectra

It should be noted that efficiency of displacement-based precedence list of ground motions varies from case to case. The eight-storey building examined herein is a good example of the first-mode dominated structure, since the plastic mechanism from the pushover analysis, were practically the same as those observed from the IDA (Fig. 8, [YouTube](#)). However, for taller buildings, which can collapse in several different modes, the efficiency of displacement-based precedence list is reduced, if the equivalent SDOF model is determined only on the basis of the pushover analysis associated with the first-mode lateral forces. For example, fifteen-storey building, which was also examined but not reported herein, can collapse in several different modes, which are significantly different as that observed from the pushover analysis. An interested reader can also check the movies showing the progression of damage in the fifteen-storey building due to pushover analysis and IDA based on ground motions ([YouTube](#)). Nevertheless, 16th, 50th and 84th percentile IDA curves of the fifteen-storey building, which were

computed on the basis of the 12 records ($s=4$) from the displacement-based precedence list, were estimated with reasonable accuracy (Fig. 9a). However, the accuracy was increased if effects of higher modes were considered in the process of determination of the precedence list (Fig. 9b). Note that the detailed description of determination of the precedence list with consideration of higher modes is beyond the scope of this paper.

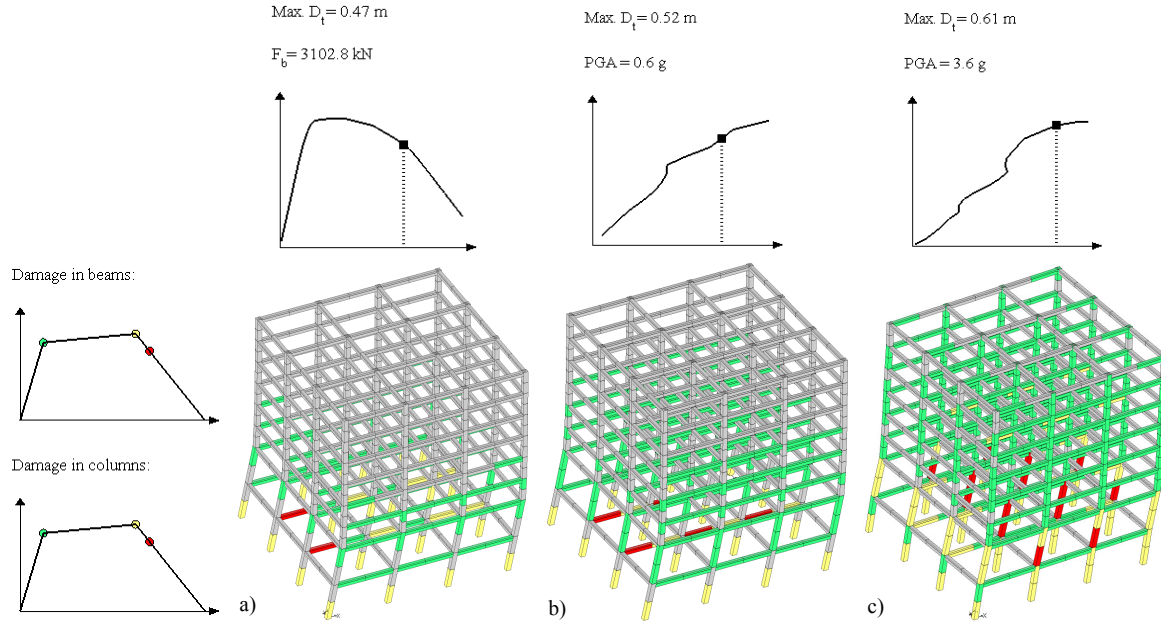


Figure 8. The deformation shape and damage distribution at the near-collapse state based on a) the pushover analysis and b) the IDA for ground motion, which caused similar damage than that observed from pushover analysis, and c) the IDA for ground motion, which caused different damage than that observed from pushover

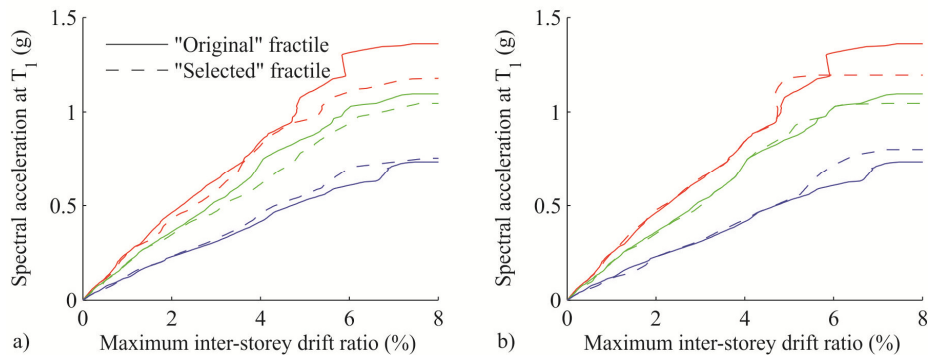


Figure 9. The “original” fractile IDA curves and the “selected” fractile IDA curves ($s=4$: 40 % of records) for the fifteen-storey building and the displacement-based precedence with consideration of a) the fundamental mode shape and b) higher-mode effects

5. CONCLUSIONS

The computational efficiency of displacement-based ground motion selection was evaluated for the eight-storey building. It was shown that 16th, 50th and 84th percentiles IDA curves can be predicted with sufficient accuracy based on only 40 % of records from the precedence list, i.e. for 12 records of all 30 records. Such reduction of computational time may help to facilitate development of iterative design procedures based on response time-history analysis.

We found that the acceleration-based precedence list of ground motions is less efficient in comparison

to the displacement-based precedence list, which was herein determined by IDA of equivalent SDOF model or by using the web-based application for prediction of approximate IDA curves. However, the efficiency of displacement-based precedence list of ground motions varies from case to case. For taller buildings, which can collapse in many different modes, the basic concept of precedence list of ground motions may not be as efficient as presented for the investigated first-mode dominated building, but the efficiency of precedence list of ground motions can be increased with consideration of effects higher modes.

ACKNOWLEDGEMENT

The results presented in this paper are based on work supported by the Slovenian Research Agency. This support is gratefully acknowledged.

REFERENCES

- Azarbakht, A., Dolšek, M. (2007). Prediction of the median IDA curve by employing a limited number of ground motion records. *Earthquake Engineering and Structural Dynamics* **36:15**,2401-2421.
- Azarbakht, A., Dolšek, M. (2011). Progressive incremental dynamic analysis for first-mode dominated structures. *Journal of Structural Engineering*. **137:3**,445-455.
- Baker, J.W. (2011). Conditional mean spectrum: Tool for ground-motion selection. *Journal of structural engineering* **137:3**,322-331.
- Bradley, B.A. (2010). A generalized conditional intensity measure approach and holistic ground-motion selection. *Earthquake Engineering and Structural Dynamics* **39:12**,1321-1342.
- CEN (2004a). Eurocode 8: Design of structures for earthquake resistance, Part 1: General rules, seismic action and rules for buildings. *EN 1998-1*. European Committee for Standardisation, Brussels, December 2004.
- CEN (2004b). Eurocode 2: Design of concrete structures, Part 1-1: General rules and rules for buildings. *EN 1992-1-1*. European Committee for Standardisation, Brussels, December 2004.
- CEN (2005). Eurocode 8: Design of structures for earthquake resistance, Part 3: Strengthening and repair of buildings. *EN 1998-3*. European Committee for Standardisation, Brussels, March 2005.
- Dolšek, M. (2010). Development of computing environment for the seismic performance assessment of reinforced concrete frames by using simplified nonlinear models. *Bulletin of Earthquake Engineering* **8:6**,1309-1329.
- Iervolino, I., Cornell, C.A. (2005). Record selection for nonlinear seismic analysis of structures. *Earthquake Spectra*, **21:3**, 685-713.
- Katsanos, E.I., Sextos, A.G., Manolis, G.D. (2010). Selection of earthquake ground motion records: A state-of-the-art review from a structural engineering perspective. *Soil Dynamics and Earthquake Engineering* **30:4**,157-169.
- Kosič M. (2010). Design of eight-storey reinforced concrete frame building according to European standard Eurocode 8. *Personal communication*, 15 December 2010.
- OpenSEES (2007). Open system for earthquake engineering simulation. Pacific Earthquake Engineering Research Center, Berkeley, California, <http://opensees.berkeley.edu>, 2007.
- Peruš, I., Poljanšek, K., Fajfar, P. (2006). Flexural deformation capacity of rectangular RC columns determined by the CAE method. *Earthquake Engineering and Structural Dynamics* **35:12**,1453-1470.
- Peruš, I., Klinc, R., Dolenc, M., Dolšek, M. (2012). A web-based methodology for the prediction of approximate IDA curves. *Earthquake Engineering and Structural Dynamics*. First published online: 3 APR 2012, DOI: 10.1002/eqe.2192.
- Vamvatsikos, D., Cornell, C.A. (2002). Incremental Dynamic Analysis. *Earthquake Engineering and Structural Dynamics*, **31:3**,491-514.
- Vamvatsikos, D., Cornell, C.A. (2006). Direct estimation of the seismic demand and capacity of oscillators with multi-linear static pushovers through IDA. *Earthquake Engineering and Structural Dynamics* **35:9**,1097-1117.